Hybrid III/V silicon photonic source with integrated 1D free-space beam steering

J. K. Doylend,* M. J. R. Heck, J. T. Bovington, J. D. Peters, M. L. Davenport, L. A. Coldren, and J. E. Bowers

Department of Electrical and Computer Engineering, University of California, Santa Barbara, California 93106, USA
**Corresponding author: doylend@ece.ucsb.edu*

Received July 31, 2012; revised September 10, 2012; accepted September 10, 2012;
posted September 11, 2012 (Doc. ID 173459); published October 9, 2012

A chip-scale optical source with integrated beam steering is demonstrated. The chip was fabricated using the hybrid silicon platform and incorporates an on-chip laser, waveguide splitter, amplifiers, phase modulators, and surface gratings to comprise an optical phased array with beam steering across a 12° field of view in one axis. Tuning of the phased array is used to achieve 1.8°(steered axis) × 0.6°(nonsteered axis) beam width with 7 dB background suppression for arbitrary beam direction within the field of view.

OCIS codes: 250.5960, 280.3640, 250.5300, 250.3140, 200.2605.

Optical phased arrays [1] have gained interest as an elegant means of nonmechanical beam steering for free-space board-to-board adaptive optical interconnects [2] and light detection and ranging (LiDAR) [3]. Fabrication of the system as an integrated photonic circuit can reduce both size and packaging complexity, and the use of silicon-on-insulator (SOI) for such an integrated device enables the incorporation of standard CMOS fabrication techniques, while also permitting hybrid integration of III-V gain materials with planar SOI waveguides for electrically pumped amplifiers [4] and single-wavelength lasers [5]. Chip-scale optical phased arrays using an off-chip laser have been reported [6–9], but eliminating external lasers and fiber coupling by integrating the laser/amplifiers on-chip is desirable.

In this work we report the first demonstration of a self-contained, steerable free-space optical source comprising an optical phased array integrated with a laser and amplifiers on-chip such that the beam can be generated, shaped, and steered in one dimension without off-chip optical components.

Design. Schematics of the device are shown in Fig. 1. A source laser was coupled to a semiconductor optical amplifier (SOA) preamplifier followed by a 1×8 multimode interferometer (MMI) splitter to separate the beam into eight channels. MMIs were used rather than a star coupler in order to minimize loss and for continuity with the previously demonstrated beam steerer reported in [9]. Each channel was then separately amplified, phase adjusted, and emitted from a surface grating array to form a beam in the far field. S-bends after the splitter separated the waveguides by 150 μm to reduce the thermal power density of the array; additional S-bends after the phase modulators reduced the separation to 5.5 μm for the grating array output. The whole device was 16 mm × 4 mm in size and was fabricated on SOI with 500 nm top silicon and 1 μm buried oxide (BOX). The rib waveguides were etched 275 nm deep and were 1 μm wide throughout most of the device, but were widened to 3 μm prior to the grating array in order to increase far field power in the main beam relative to the side lobes [10]. The surface gratings were separately etched 50 nm deep with 550 nm pitch and 20% duty cycle in order to distribute the emission along the full 200 μm length of the grating array, thus maintaining a narrow beam in the far field along the longitudinal θ axis (i.e., parallel to the waveguides) [9]. The waveguides within the grating array were arranged with 5.5 μm pitch for a total array lateral dimension of 44 μm; these dimensions were chosen in order to maintain overall beam width in the lateral ϕ axis (i.e., perpendicular to the waveguides) of 1.8° while keeping the side lobes outside of the 12° field of view.

Fabrication. Rib waveguides were photolithographically defined and etched in SOI, after which phase modulator diodes were produced within the top silicon via ion implantation of boron and phosphorus. These phase modulators were operated in forward bias to provide local heating to the waveguide, thus thermo-optically adjusting the effective index of the guided mode. Trenches between the phase modulators were etched to the BOX to improve thermal isolation. Following a high-temperature dopant anneal, gratings were patterned using e-beam lithography. III-V quantum well laser material was wafer-bonded to the SOI and the laser and SOA mesas were then patterned and etched, with metal contacts defined by e-beam evaporation and liftoff. Hard-baked SU8 photoresist and PECVD SiO_2 were used as buffer layers over the waveguides with vias etched through them prior to probe-pad metal e-beam evaporation and lift off.

Results. The phase tuning efficiency was measured by recording the far field pattern produced by adjacent pairs of channels as phase was tuned, and was determined to be 97 mW/π, similar to what has been observed for conventional heaters overlaying silicon rib waveguides with the same BOX thickness [11]. With the laser and

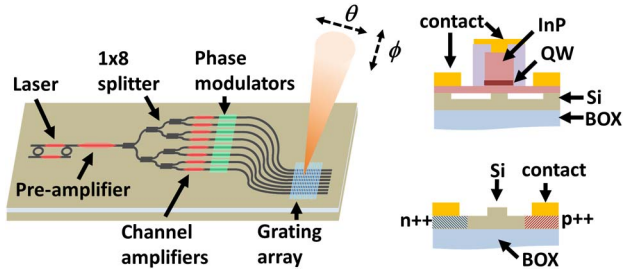

Fig. 1. (Color online) Schematics (not to scale) of the overall device (left), cross-section of the gain elements (right top), and cross-section of the phase modulators (right bottom). QW = quantum wells, Si = silicon, BOX = buried oxide.

preamplifier each pumped at 250 mA, each channel's SOA was individually turned on and its current adjusted for uniform power output to the far field. One of the eight waveguides (channel 5) was found to be damaged such that no signal power could be attained from its SOA; this channel was therefore turned off and only the remaining seven were used to produce the beam.

With seven channels biased for uniform optical output (pump currents ranged from 107 to 163 mA) and the chip mounted on a stage held at 18 °C, current in the SOAs and phase tuners was cycled at 125 Hz, 20% duty cycle (1.6 ms dwells) in order to reduce on-chip heating from the phase tuners. The preamplifier current was cycled at 10% duty cycle (0.8 ms dwells) with a 0.8 ms delay relative to the other elements in order to blank the beam while the SOAs and phase modulators were being turned on and adjusted. A far field imaging system together with a LabVIEW feedback control algorithm similar to that described in [9] were used to adjust the relative phases for shaping and pointing the beam across a 12° range at 1° increments. These phase settings were then used in a lookup table such that the beam could be steered without external feedback, and were found to be stable over several days (the requirement for occasional recalculation was attributed to changes in the thermal contact between the chip and the stage, which can be mitigated by soldering); this stability is a benefit of eliminating optical alignment through integration.

With constant preamplifier current, beam power varied by 3.2 dB across the steering range due to variations in overall heating at each phase setting (and thus SOA gain); it was found that varying preamplifier current from 245 to 290 mA provided 3.4 dB power adjustment without measurable detriment to beam width or background suppression, and is therefore sufficient to compensate for variations in far field output versus steering angle. The normalized far field beam profiles in the ϕ axis are shown in Fig. 2 together with the dependence of beam power on steering angle and preamplifier current. Beam position accuracy of 0.3° was achieved with background suppression of >7 dB for all solved beam positions (the theoretical best background suppression with channel 5 switched off was 8.4 dB). The beam cross-section in both axes for the $\phi = 0°$ case is shown in Fig. 3.

The modeled beam profile in θ was calculated using scattering propagation constant $\alpha = 164\ \mathrm{cm}^{-1}$, which was measured by imaging the scattered intensity versus propagation length along the grating in the near field. Full width half-maximum (FWHM) beam width was measured to be 1.8° in ϕ and 0.6° in θ. The discrepancy between the modeled and measured beam width in θ was attributed to mode evolution within the grating.

Using the solved lookup table to steer the beam to a photodetector positioned in the far field (8 cm distance), beam power with 250 mA pre-amplifier current was measured to be 4.1 μW (quasi-cw), which is comparable to that achievable with the passive chip reported in [9] using an off-chip 1 mW fiber-coupled laser, although 6 dB lower than that required for a commercially viable board-to-board adaptive interconnect [2]. The on-chip laser output was measured by operating the preamplifier in reverse bias as a photodiode. For 250 mA laser current and –3 V preamplifier bias, 66 μA photocurrent was measured

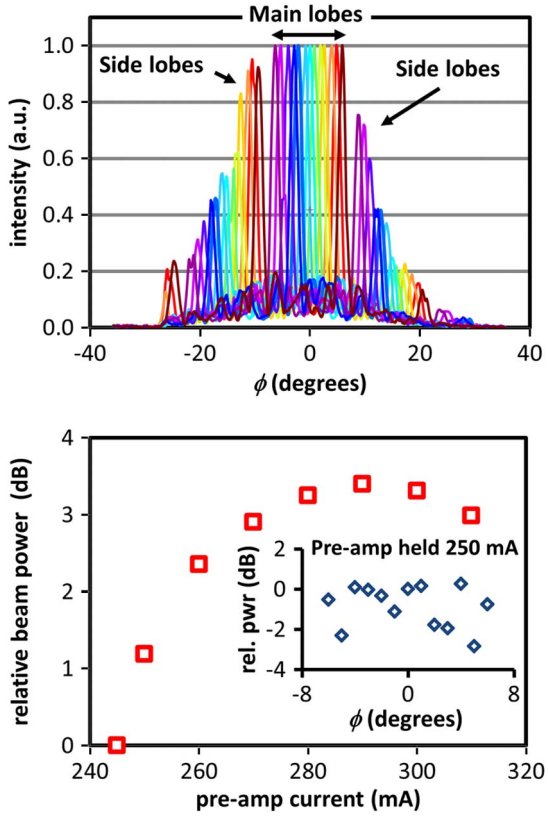

Fig. 2. (Color online) Normalized far field beam cross-sections measured for beam positions from $\phi = -6°$ to $\phi = 6°$ at 1° increments (top), and relative beam power measured versus preamplifier current (bottom). The inset shows variation of beam power with steering angle for constant preamplifier current.

indicating on-chip laser power of 110 μW for photodiode responsivity of 0.6 A/W.

By calculating the power lost to side lobes (–6.6 dB), backside emission from the grating (–6.3 dB), excess loss in the 1×8 MMI tree (–3 dB corresponding to measured –1 dB per splitter [9]), and propagation loss (–4.8 dB) the amplifying elements are estimated to provide 6.4 dB gain.

The beam energy required for short-range (i.e., <2 km) imaging LiDAR is at least 15 μJ [12]; the output power limitation observed in this work was attributed to on-chip heating. This can be mitigated by introducing thermal shunts through the BOX, soldering the chip to a heat sink, and employing electro-optic rather than thermo-optic phase modulation.

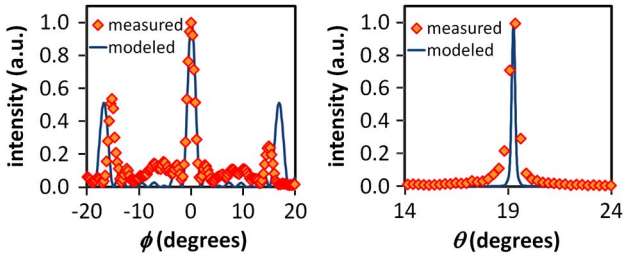

Fig. 3. (Color online) Measured far-field beam cross-sections in ϕ (left) and θ (right) of the far field beam for the phased-array solution at $\phi = 0°$. The discrepancy between measured and modeled side-lobe position was attributed to lens Seidel aberrations.

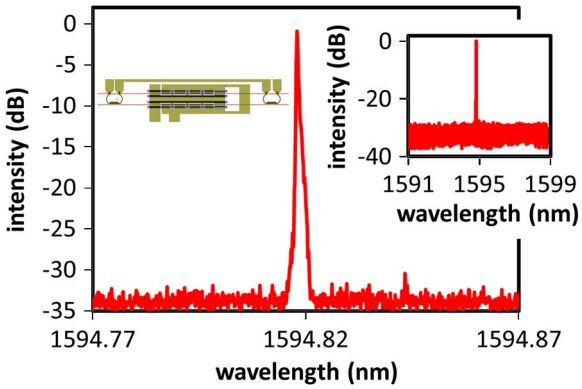

Fig. 4. (Color online) Optical spectrum (resolution: 40 MHz) of the free-space ouput demonstrating single wavelength operation (inset: right) from the on-chip source laser (inset: left).

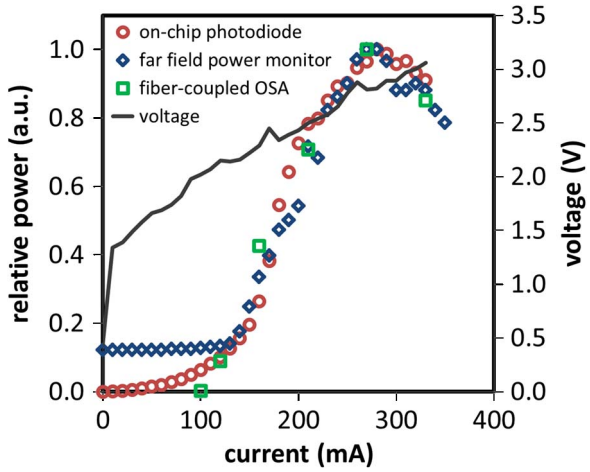

Fig. 5. (Color online) Normalized measurements of (a) the on-chip photocurrent from the preamplifier held at −3 V bias, (b) power coupled to a Newport 818 power meter using the far field imaging system, and (c) peak signal fiber-coupled to the APEX 2541 OSA.

The source laser incorporated a dual ring-coupled cavity similar to the design described in [13] to provide single-wavelength operation. The spectral characteristics of the laser were measured with an APEX 2051A optical spectrum analyzer by collecting the free-space optical output from the combined laser/preamplifier/SOA. The beam spectrum thus obtained is shown in Fig. 4. Laser linewidth was less than 40 MHz with 30 dB sidemode suppression. Since the laser in the device was integrated with amplifiers, the LIV characteristic was measured indirectly: (a) by operating the preamplifier in reverse bias (−3 V) to act as a photodiode, (b) by using the imaging lens system to measure the optical power versus on-chip laser current while holding/pulsing the SOAs as described above, and (c) by recording the signal strength of the laser peak on the optical spectrum analyzer (OSA). These data represent power at different stages in the on-chip link budget and are therefore shown normalized in Fig. 5.

The nonzero emitted power for the far field power monitor measurement was due to amplified stimulated emission (ASE) emitted from the amplifier array during the 800 μs delay between SOA and preamplifier turn-on. The laser exhibited threshold current of 120 mA corresponding to 2.0 kA/cm^2 threshold current density, which is comparable to other CW single-wavelength hybrid lasers [5].

Conclusion. A hybrid silicon photonic integrated circuit phased array incorporating a laser, amplifiers, and individual phase tuning for free-space beam steering has been demonstrated, achieving 12° tuning range in the far field with 4.1 μW main lobe beam power, 7 dB background suppression, and 0.3° pointing accuracy. Future work will incorporate wavelength tuning of the laser for two-dimensional steering, on-chip interferometers, and photodiodes for internal feedback concerning the far field beam shape, a larger emission array for improved far field spatial resolution, and electro-optic phase modulation for high-speed beam steering.

The authors thank Pietro Binetti, Weihua Guo, Chad Althouse, and Scott Rodgers for useful discussions. This research was supported by the DARPA Sweeper program, grant no. HR0011-10-2-0003. Jonathan Doylend's work was supported in part by a Natural Sciences and Engineering Research Council of Canada Post-doctoral Fellowship.

References

1. P. F. McManamon, P. J. Bos, M. K. Escuti, J. Heikenfeld, S. Serati, X. Huikai, and E. A. Watson, Proc. IEEE **97**, 1078 (2009).
2. C. J. Henderson, D. G. Leyva, and T. D. Wilkinson, J. Lightwave Technol. **24**, 1989 (2006).
3. A. Schweinsberg, Z. Shi, J. E. Vornehm, and R. W. Boyd, Opt. Express **19**, 15760 (2011).
4. H. Park, Y.-H. Kuo, A. W. Fang, R. Jones, O. Cohen, M. J. Paniccia, and J. E. Bowers, IEEE Photon. Technol. Lett. **19**, 230 (2007).
5. A. W. Fang, M. N. Sysak, B. R. Koch, R. Jones, E. Lively, Y. Kuo, D. Liang, O. Raday, and J. E. Bowers, IEEE J. Sel. Top. Quantum. Electron. **15**, 535 (2009).
6. K. Van Acoleyen, W. Bogaerts, J. Jágerská, N. Le Thomas, R. Houdré, and R. Baets, Opt. Lett. **34**, 1477 (2009).
7. K. Van Acoleyen, H. Rogier, and R. Baets, Opt. Express **18**, 13655 (2010).
8. D. Kwong, A. Hosseini, Y. Zhang, and R. T. Chen, Appl. Phys. Lett. **99**, 051104 (2011).
9. J. K. Doylend, M. J. R. Heck, J. T. Bovington, J. D. Peters, L. A. Coldren, and J. E. Bowers, Opt. Express **19**, 21595 (2011).
10. J. K. Doylend, M. J. R. Heck, J. T. Bovington, J. D. Peters, and J. E. Bowers, in *Optical Fiber Communication Conference*, OSA Technical Digest Series (Optical Society of America, 2012), paper OM2J.1.
11. R. Jones, J. K. Doylend, P. Ebrahimi, S. Ayotte, O. Raday, and O. Cohen, Opt. Express **15**, 15836 (2007).
12. J. A. Overbeck, M. S. Salisbury, M. B. Mark, and E. A. Watson, Appl. Opt. **34**, 7724 (1995).
13. B. Liu, A. Shakouri, and J. E. Bowers, IEEE Photon. Technol. Lett. **14**, 600 (2002).